

# Recent advances in drug delivery applications of aqueous two-phase systems

Mojhdeh Baghbanbashi <sup>a</sup>, Hadi Shaker Shiran <sup>b</sup>, Ashok Kakkar <sup>c</sup>, Gholamreza Pazuki <sup>b</sup> and Kurt Ristroph <sup>a,\*</sup>

<sup>a</sup>Department of Agricultural and Biological Engineering, Purdue University, 610 Purdue Mall, West Lafayette, IN 47907, USA

<sup>b</sup>Department of Chemical Engineering, Amirkabir University of Technology (Tehran Polytechnic), Tehran 1591634311, Iran

<sup>c</sup>Department of Chemistry, McGill University, 801 Sherbrooke St West, Montreal, QC H3A 0B8, Canada

\*To whom correspondence should be addressed: Email: [ristroph@purdue.edu](mailto:ristroph@purdue.edu)

Edited By: Rui Reis

## Abstract

Aqueous two-phase systems (ATPSs) are liquid–liquid equilibria between two aqueous phases that usually contain over 70% water content each, which results in a nontoxic organic solvent-free environment for biological compounds and biomolecules. ATPSs have attracted significant interest in applications for formulating carriers (microparticles, nanoparticles, hydrogels, and polymersomes) which can be prepared using the spontaneous phase separation of ATPSs as a driving force, and loaded with a wide range of bioactive materials, including small molecule drugs, proteins, and cells, for delivery applications. This review provides a detailed analysis of various ATPSs, including strategies employed for particle formation, polymerization of droplets in ATPSs, phase-guided block copolymer assemblies, and stimulus-responsive carriers. Processes for loading various bioactive payloads are discussed, and applications of these systems for drug delivery are summarized and discussed.

**Keywords:** aqueous two-phase system, drug delivery, nanoparticle, microparticle, stimuli-responsive carrier

## Introduction

### Aqueous two-phase system overview

Aqueous two-phase systems (ATPSs) are liquid–liquid phase equilibria between two aqueous phases that are formed when the concentration of hydrophilic solutes in solution exceeds a critical concentration (Fig. 1). Due to immiscibility of the solutes at this concentration, phase separation occurs (1–4) in such a way that each aqueous phase is rich in one of the phase-forming compounds (5). Martinus Beijerinck first recognized the ATPS phenomenon in 1896 while preparing an aqueous solution of concentrated starch and gelatin in water for bacterial cultivation (4, 6), and Per-Åke Albertsson utilized an ATPS for the first time to separate proteins, viruses, cells, and cell fragments using the preferential distribution of components between the two aqueous phases (2, 4, 6).

The ATPS approach brings two main advantages to biomaterial processing. First, because each of the two phases formed typically contains over 70% water by volume, utilizing this approach for biological materials is an attractive alternative to liquid–liquid extraction or fractionation processes that utilize organic solvents. Each phase in a two-phase ATPS provides a biocompatible environment (1, 2, 7, 8) that does not cause protein denaturation, stabilizes cells, and preserves biological activity (3, 5, 9). Beyond water content, another reason for biocompatibility is the low interfacial tension in aqueous–aqueous systems—about  $10^{-4}$ – $10^{-1}$  dyne/cm, which is significantly lower than water–oil systems (4, 8, 9). The aqueous–aqueous interface provides a large contact surface in the dispersed

phase, which is permeable and allows the diffusion and exchange of solvents and small molecules between the two phases (4, 5, 9).

The second advantage is that an ATPS can simultaneously accomplish multiple operations—separation, concentration, and purification—that would otherwise require individual unit operations (1, 7, 9). This contributes to the overall scalability of the approach (2, 3, 5, 9), which uses chemicals and equipment that are common and straightforward to use (5). As mentioned above, reduction in organic solvent compared with liquid–liquid extractions is advantageous from an environmental perspective.

Limitations to the ATPS approach include lack of specificity, which can be improved to some extent by manipulating composition, temperature, and other process parameters (10). Some parameters, such as high cost of some compounds used in ATPSs, high concentration of phase-forming components, such as salts in one phase, and high viscosity of polymer/polymer-based ATPSs, can limit applications to certain materials (3, 11). These are discussed in more detail below.

### Types of ATPSs, applications other than drug delivery, and scope of the review

Several combinations of solutes have been reported to form ATPSs (12). The most common are those based on polymer/polymer (13–16), polymer-salt (17–20), low molecular weight alcohols/salt (21–23), ionic liquid/salt (24–26), deep eutectic solvent/salt (27–30), and micellar ATPSs (31–35). Examples of phase-forming

**Competing Interest:** The authors declare no competing interests.

**Received:** May 31, 2024. **Accepted:** June 6, 2024

© The Author(s) 2024. Published by Oxford University Press on behalf of National Academy of Sciences. This is an Open Access article distributed under the terms of the Creative Commons Attribution-NonCommercial License (<https://creativecommons.org/licenses/by-nc/4.0/>), which permits non-commercial re-use, distribution, and reproduction in any medium, provided the original work is properly cited. For commercial re-use, please contact [reprints@oup.com](mailto:reprints@oup.com) for reprints and translation rights for reprints. All other permissions can be obtained through our RightsLink service via the Permissions link on the article page on our site—for further information please contact [journals.permissions@oup.com](mailto:journals.permissions@oup.com).

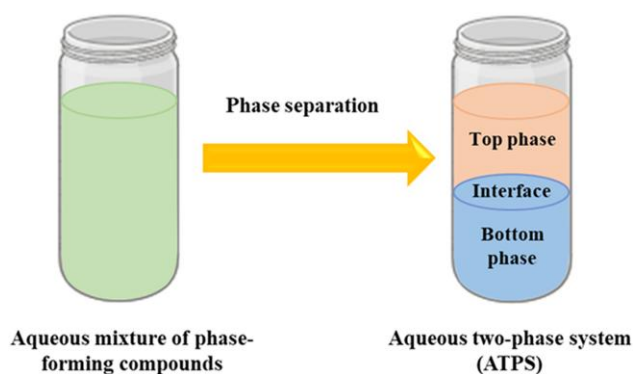


Fig. 1. Schematic representation of ATPS.

compounds used in these ATPSs are reported in Table S1. Brief descriptions and advantages/disadvantages of these classes are provided in the [Supporting Information](#).

The distinct characteristics of ATPSs have led to interest in their application in a variety of fields, including the pharmaceutical, food, and chemical industries. The conventional applications of ATPSs are process based, e.g. utilizing these systems in separation, extraction, enrichment, and purification of drugs (36–40), vitamins (41–44), proteins (45–49), cells and organelles (50–54), enzymes (55–59), carbon nanotubes (60–63), and metal ions (64–69). ATPSs have also been used for biomedical applications, including neuronal cell differentiation (70), microprinting (71), as well as particle reactor preparation (72).

The focus of this review is the application of ATPSs for the formulation of carriers, such as micro/nanoparticles, hydrogels, microcapsules, micelles, and polymersomes for drug delivery or cell therapy purposes, where the unique benefits offered by these systems in biological media have warranted significant research. After an overview of the basic principles of ATPS preparation, such as the construction of a binodal curve to determine the two-phase region and compound partitioning, we discuss different strategies used to prepare particles using ATPSs, and an analysis of how these particles perform as carriers of pharmaceuticals and cells for drug delivery and cell therapy purposes. The benefits of binding chemical entities sensitive to endogenous or exogenous stimuli in the structure of these carriers are also discussed. A schematic representation of the scope of this review is shown in Fig. 2.

## ATPS formation, thermodynamics, and phase diagrams

The equilibrium between gravitational, flotation, and frictional forces leads to phase separation in ATPSs (7, 8, 73, 74). When two components in an aqueous solution form an ATPS, three regions with unique features are formed: two liquid phases (top and bottom) and their interface (Fig. 1). Thermodynamically, the Gibbs free energy of the system ( $G$ ) depends on enthalpy ( $H$ ) and entropy ( $S$ ) contributions ( $\Delta G = \Delta H - T\Delta S$ ). If  $\Delta G$  is  $<0$ , the mixing process is spontaneous, and no phase separation occurs. If the entropic contribution is smaller than the enthalpy contribution,  $\Delta G > 0$ , and the mixing process is not spontaneous, a biphasic system will form (4, 6). The biphasic region is unique to each system under specific conditions, such as pH and temperature (2, 7). The boundary between the concentrations of the two- and single-phase regions is called the binodal curve and is a function of the concentration of the two components that constitute the ATPS. A schematic phase diagram is shown in Fig. S1. A typical phase diagram provides

information such as the concentration of (i) components required to form an ATPS, and (ii) components in the upper and lower phases; as well as the volume ratio of the phases (2, 5). The concepts depicted in a phase diagram, and the procedure for driving a binodal curve for an ATPS is discussed in the [Supporting Information](#).

Several factors affect phase separation in an ATPS (7, 8, 75). The interactions among components within an aqueous solution, including hydrophobic/hydrophilic interactions, hydrogen bonding, van der Waals forces, and electrostatic interactions, dictate the aggregation of components and promote the formation of separate phases as the system achieves an energetically favorable state (74, 76, 77). Hydrophobic/hydrophilic interactions are of the main factors in phase separation, as the hydrophobic regions of the phase-forming components repel water molecules, while the hydrophilic regions/components interact favorably with water. This variation in water affinity prompts the formation of ATPS, with hydrophobic components preferentially partitioning into one phase and hydrophilic components into the other (78, 79). The molecular weight and concentration of phase-forming components, particularly polymers, have a significant influence over phase separation dynamics (80, 81). Increasing polymer molecular weight and concentration can enhance polymer hydrophobicity and capacity to form more extensive aggregates, resulting in the creation of a stable ATPS (20, 82). In ATPSs containing salt as a phase-forming component, salt concentration and type modify the ionic strength and solvation properties of the system. Different salts exhibit distinct salting in/salting-out properties and impact the system's osmotic pressure, thereby altering phase behavior (83, 84). Temperature also significantly influences ATPS phase separation by modulating the strength of molecular interactions, density, solubility, and intermolecular forces, consequently affecting phase equilibria (80, 81, 85). pH alterations can change the charge state of system molecules, while the ionization of salts can modify ionic strength and electrostatic interactions, influencing solvation properties, and molecule partitioning between phases (82, 86). A comprehensive understanding of these factors is imperative for effectively designing and optimizing ATPSs for diverse applications.

The selective distribution of compounds between the two phases of an ATPS, known as partitioning, occurs when the molecules of an added compound to the system exhibit a tendency to be in one of the phases after equilibrium. It can be described with a partition coefficient ( $K$ ), the ratio of the concentration of the substance in the top phase to that in the bottom phase. The main factors known to influence partitioning are the characteristics of the ATPS—molecular weight and concentration of the components, presence of hydrophobic groups, ionic strength, pH, and temperature—and interactions between a compound and the phase to which it partitions—van der Waals forces, hydrogen bonding, electrostatic interactions, and structural interactions (5, 6, 8, 9, 87). As an example, we recently investigated the partitioning of curcumin as an antiinflammatory drug in a suite of polymer-salt ATPSs (20), varying the polymer and salt type, polymer molecular weight, and temperature. The hydrophobicity of the polymer phase increased as polymer molecular weight was increased, and this in turn improved the partitioning of curcumin into that phase. Polymer composition—i.e. utilizing polyethylene glycol (PEG) versus polypropylene glycol 400 (PPG) or a three-block copolymer of PEG–PPG (Pluronic L35) affected partitioning. Finally, ATPSs formed using salts with greater salting-out effect and at higher temperatures partitioned curcumin more efficiently than salts with lower salting-out effect and lower temperatures.

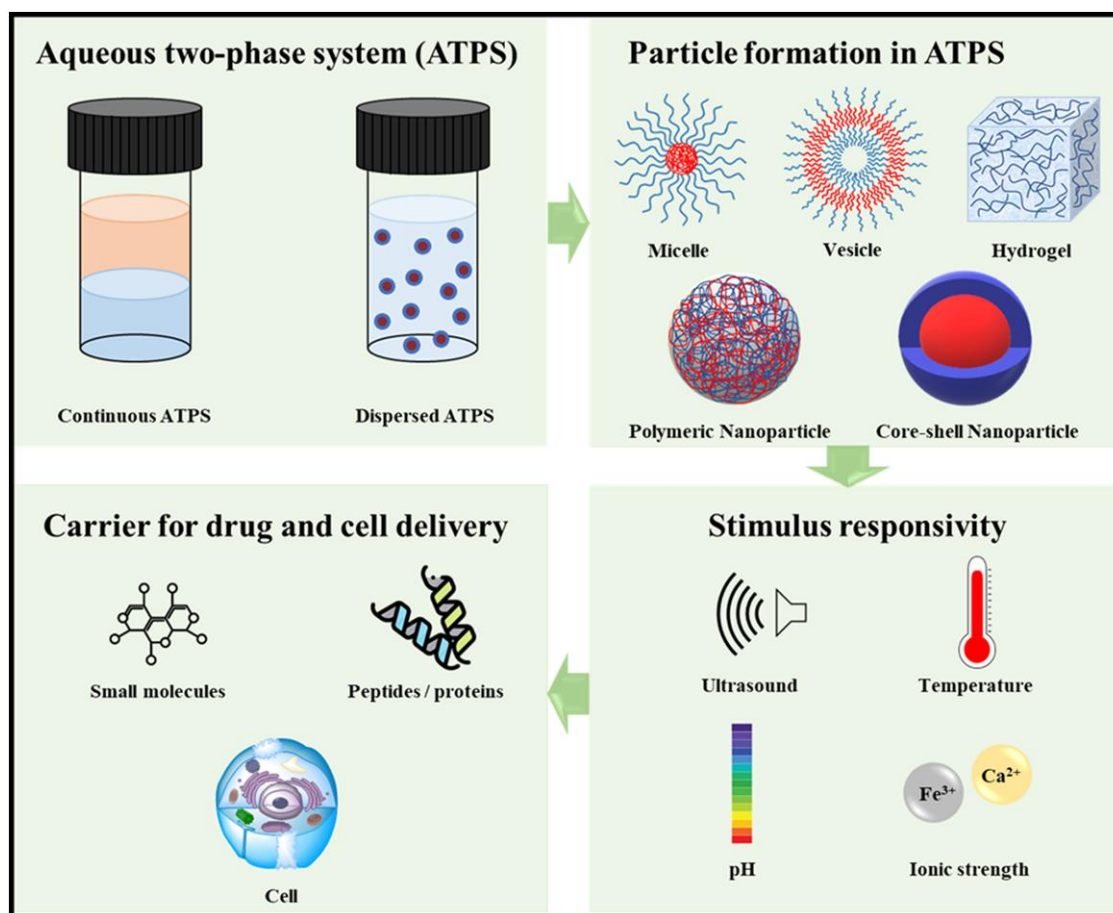


**Fig. 2.** Schematic illustration of an ATPS, various particles made using ATPSs, their current application as carriers, and the stimuli used in these carriers.

We will describe below two examples as an illustration. Using the ATPS approach, Ahsaie and Pazuki (88) studied separation of 6-aminopenicillanic acid (6-APA) from phenyl acetic acid (PAA), which is a byproduct in the preparation of 6-APA. A suite of copolymer-salt ATPSs were prepared using Pluronic 10R5, Pluronic L35, or PEG-ran-PPG as the copolymers and tri-sodium citrate, tri-potassium citrate, di-potassium phosphate, sodium sulfate, or magnesium sulfate as salts. Block copolymers showed a larger biphasic region compared with random copolymers. The same results were obtained for sodium sulfate, due to its higher salting-out effect compared with the other studied salts. In partitioning studies, PAA tended to the copolymer phase ( $K > 1$ ), and the partition coefficient for 6-APA was around 1; the selectivity of Pluronic 10R5/sodium sulfate ATPS employed for separation of 6-APA and PAA was found to be 53.

Domingues et al. (89) used polymer-salt ATPSs consisting of polymers, PEG, Pluronic L35 or Pluronic L64, and salts  $\text{Na}_2\text{SO}_4$ ,  $\text{Li}_2\text{SO}_4$ ,  $\text{MgSO}_4$ ,  $\text{Na}_2\text{C}_4\text{H}_4\text{O}_6$ , or  $\text{Na}_3\text{C}_6\text{H}_5\text{O}_7$  to study the extraction of steroid hormones present in four medicines: Minesse, Ciclo 21, Diane 35, and Mesigyna. The hydrophobic hormones partitioned to the polymer-rich top phase to different extents depending on the solubility of each compound in different polymers, and the use of sulfate-based salts improved this separation due to their high salting-out ability.

## Particle formulation and stabilization

Due to the advantages discussed above, the ATPS approach has been employed for the formation of microcapsules, hydrogels,

etc., as an alternative to methods such as electrohydrodynamic jetting (90), co-extrusion (91), and water-oil biphasic emulsions (92), which suffer from low hydrophilic cargo encapsulation, particle deformation, nonuniform particle morphology, extensive use of organic solvents, and incompatibility with biological systems (93–95). As mentioned earlier, ATPS parameters such as mixture point and polymer molecular weights must be carefully selected to control biphasic stability, phase viscosity, compatibility and partitioning of added compounds (cargo, polymerization initiator, dyes, etc.), and droplet formation speed (96–99).

Several carriers, including micro- and nanoparticles (95, 100, 101), hydrogels (102–104), and polymersomes (105), have been prepared using ATPSs. Various techniques have been employed to create aqueous droplets within these systems (106). Droplets can be produced either by mechanically stirring the ATPS or by adding an aqueous solution of one ATPS component into another component's solution while stirring (94, 95, 107). Sonication has also been utilized to generate submicron-sized droplets (96). Microfluidic devices are another technique used to form droplets for a range of applications (4, 97, 103, 108, 109). In this method, the dispersed phase of one ATPS component is injected into the continuous phase of another, forming droplets within the microfluidic device channel. The size and morphology of these droplets can be fine-tuned by manipulating factors such as the composition and concentration of the ATPS (94, 96), stirring speed (94), concentrations of additives (95, 100), flow rates, and the volume ratio of ATPS components (103, 108, 109), as well as by crosslinking ATPS components (94, 96, 107).

**Table 1.** Summary of the most common strategies applied for carrier formation in ATPS.

Particle formation strategy	Description	Reference
ATPS-guided particle formation	Partitioning of a compound in an ATPS and formation of micro/nanoparticles based on interactions among components	95, 100
Polymerization of droplets in ATPS	Photopolymerization of acrylate functional groups on one of the phase-forming compounds in the presence of photoinitiator and UV light Crosslinking the aqueous droplets by ionic bonding between sodium alginate and Ca <sup>2+</sup> ions Formation of linkers between compounds present in the ATPS droplets using coupling reactions and thiol-ene and thiol-yne click reactions	94, 96, 98, 102, 103, 107, 108, 110 87, 97, 109, 111, 112 93, 113, 114
Phase-guided block copolymers assemblies	Self-assembly of block copolymers into micellar or vesicular assemblies via addition of them to an ATPS or application of them for ATPS formation	40, 105, 115, 116

Different strategies that were employed to make drug carriers in ATPSs are included into three categories: (i) ATPS-guided particle formation, (ii) polymerization of droplets in an ATPS, and (iii) phase-guided block copolymer assemblies. These are briefly summarized in Table 1 and described in detail below.

### ATPS-guided particle formation

One method of particle formation is to add a copolymer or nanoparticle into an ATPS; the added material partitions into one phase based on its interactions with ATPS components, and this process can be used to load biomolecular payloads into the resulting particles. Yeredla et al. (95) utilized a Pluronic F127/dextran ATPS to prepare microparticles for drug delivery applications. Pluronic F127 is a triblock copolymer with a molecular weight of 12,600 Da, containing 70% PEG and 30% PPG and which shows thermo-responsive behavior. At temperatures higher than the critical micelle temperature of Pluronic F127 in the presence of dextran, an ATPS is formed. Microparticles were prepared by adding poly(lactide-co-glycolide) (PLGA) to the ATPS while stirring. Due to the hydrophobicity of PLGA, it partitioned to the Pluronic F127-rich phase, which was dispersed in a continuous dextran phase. This resulted in ATPS-guided self-assembly of the polymers into microparticles in the size range of 2–10 μm. Three-color fluorescent micrographs of the microparticles (Fig. 3) showed that Pluronic F127 was concentrated in the core of the microparticle, while dextran forms a concentrated shell around it, and PLGA constitutes the backbone matrix. Increasing the concentration of PLGA altered the morphology of the particles and led to the formation of polymer-blended composite structures due to the insertion of more dextran into the dispersed Pluronic F127/PLGA phase, which triggered the formation of multiple emulsions in the dispersed phase (95).

In a recent study (100), silica-based nanocarriers were prepared using a PEG/lysine ATPS that could partition doxorubicin more efficiently than previously reported ATPSs (117). The addition of silica nanoparticles (SiO<sub>2</sub>) to the ATPS resulted in the surface modification of SiO<sub>2</sub>; the silanol groups on the surface of SiO<sub>2</sub> formed hydrogen bonds with the ethereal oxygen atoms as well as terminal hydroxy groups of PEG and amine groups of lysine, as confirmed using fourier transform infrared spectroscopy and thermogravimetric analysis. A size increase of the SiO<sub>2</sub> nanoparticles after addition into the ATPS was observed by transmission electron microscopy, corroborating nanocarrier loading and surface modification.

### Polymerization of droplets in an ATPS

For aqueous droplets formed in an ATPS to be stabilized as microparticles, either the droplet core or an outer surface layer, must be

solidified to prevent coalescence. One solidification technique is polymerization of a crosslinked polymer in the core or on the droplet surface. Various crosslinking methods have been employed for droplet stabilization, including ultraviolet (UV) light irradiation, heating, using radical initiators for polymerization, and click chemistry (93, 118). The three most common crosslinking methods employed for droplets formed in ATPSs without the need for organic solvents are summarized below.

#### Photopolymerization of acrylate functional groups

In this method, at least one of the phase-forming polymers is functionalized with acrylates, which can be polymerized in the presence of a photoinitiator and UV light. During polymerization, the acrylate groups react with other acrylates next to them on the same polymer (Scheme 1A) or, the groups on other polymeric macromolecules (Scheme 1B), which leads to the formation of a crosslinked polymeric network.

Several examples follow. Neffe et al. (94) applied a gelatin/dextran ATPS (water/water emulsion) as an alternative to a water–oil emulsion for the preparation of microparticles for cell encapsulation. They functionalized the amine groups of gelatin using glycidyl methacrylate (GMA) to prepare GMA-gelatin, which formed an ATPS with dextran. By stirring the ATPS, GMA-gelatin droplets were formed in the continuous dextran phase (Fig. 4A). The methacrylate groups on GMA-gelatin were photopolymerized by irradiation, and a polymeric matrix of gelatin was obtained (Fig. 4B). Particle character and the viability of the encapsulated cells varied with dextran molar mass, ATPS mixture point, stirring speed, and irradiation time. The irradiation duration was selected as 60 s in this study, and to improve the photopolymerization efficacy during time duration, irgacure 2959 was added to the system as a photoinitiator.

Ma et al. (108) fabricated microparticles with complex shapes, utilizing UV-induced polymerization of acrylate groups of an ATPS in simple single-emulsion microdroplets prepared in a poly(dimethylsiloxane)-based microfluidic device. The dextran inlet of the microfluidic device was inserted into poly(ethylene glycol) diacrylate (PEGDA) flow containing irgacure 2959 photoinitiator. The phase separation of the ATPS consisting of dextran and photopolymerizable PEGDA led to the formation of core (dextran)-shell (PEGDA) microdroplets, which formed microgel particles upon exposure to UV. Variations in the flow rate of the phases were found to control the size and shape of the particles (108).

Okur et al. (107) prepared functionalized PEG hydrogel nanoparticles by using a prepolymer PEG solution in which one of the acrylate functional groups of PEGDA was covalently bound to the thiol group of CREKA peptide (cysteine–arginine–glutamic acid–lysine–alanine). Photocrosslinking initiator (eosin Y), co-initiator (triethanolamine, TEA), and accelerator (1-vinyl-2-pyrrolidone)

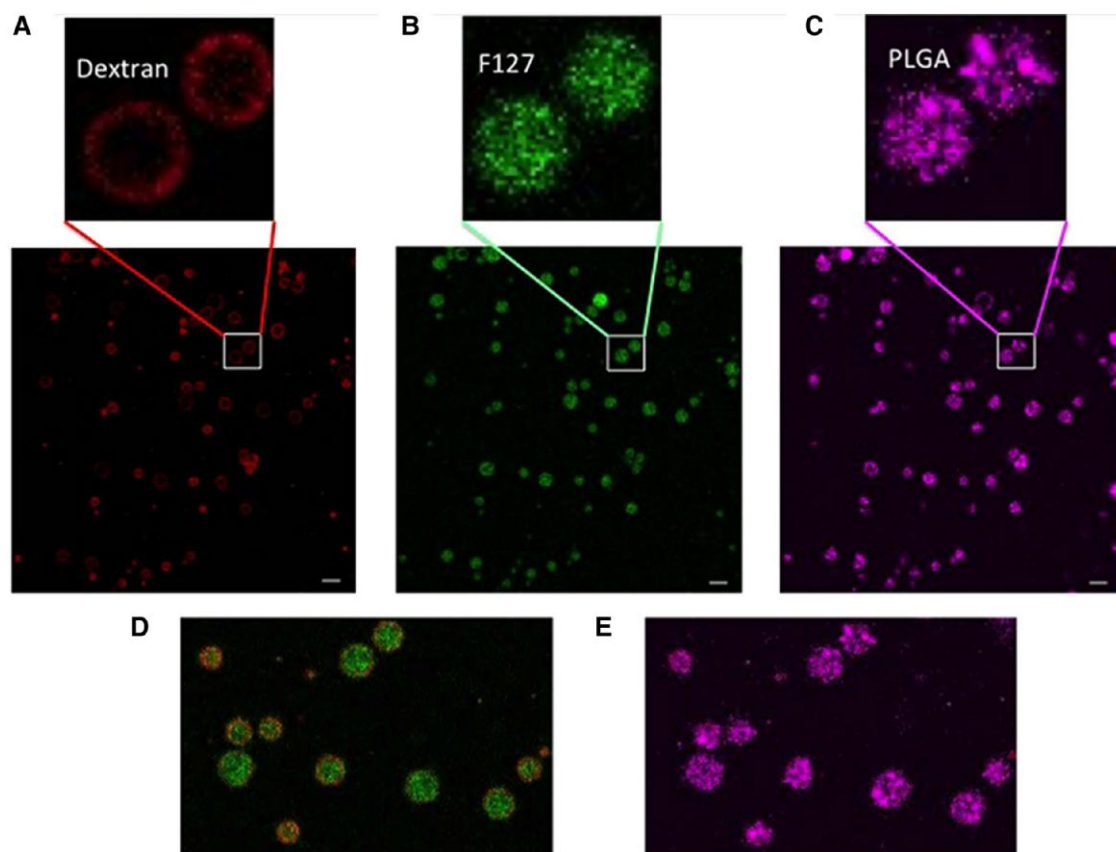


**Fig. 3.** The confocal microscopic images of the obtained microparticles in the Pluronic F127/ dextran ATPS in the presence of PLGA (0.0625% Cy5-PLGA, 2% fluorescein isothiocyanate (FITC)-pluronic/10% TRITC-dextran). A) TRITC-dextran, B) FITC-Pluronic F127, C) Cy5-PLGA, D) Pluronic F127-dextran core-shell morphology of particles, and E) PLGA backbone matrix. Scale bar 10  $\mu\text{m}$ . Reproduced with permission from Ref. (95).

were added to the prepolymer solution. Upon mixing with a dextran phase, the droplets were covalently crosslinked when exposed to green light, leading to the formation of submicron-sized hydrogel particles. In another study, Liu et al. (103) reported self-orienting crescent-shaped hydrogel microparticles produced using a PEG/dextran ATPS-based microfluidic device and photocrosslinking. Dextran aqueous phase containing cyclo(Arg-Gly-Asp-D-Phe-Cys) (RGD) peptide for functionalizing the inner surface of the particles, PEGDA aqueous phase with the photoinitiator (lithium phenyl-2,4,6-trimethyl-benzoyl phosphinate), and the surfactant solution in hexadecane were the inner, middle, and oil phases of the microfluidic device, respectively. These phases were injected into the device separately, and the acrylates of obtained microdroplets were crosslinked through UV irradiation. The hexadecane phase was removed by washing, and pouring the crescent-shaped hydrogel microparticles into a petri dish led to the spontaneous orientation of the microparticles due to the gravitational force while settling, as illustrated in Fig. S2A. This behavior provides means to control the microparticles as cell carriers (Fig. S2B).

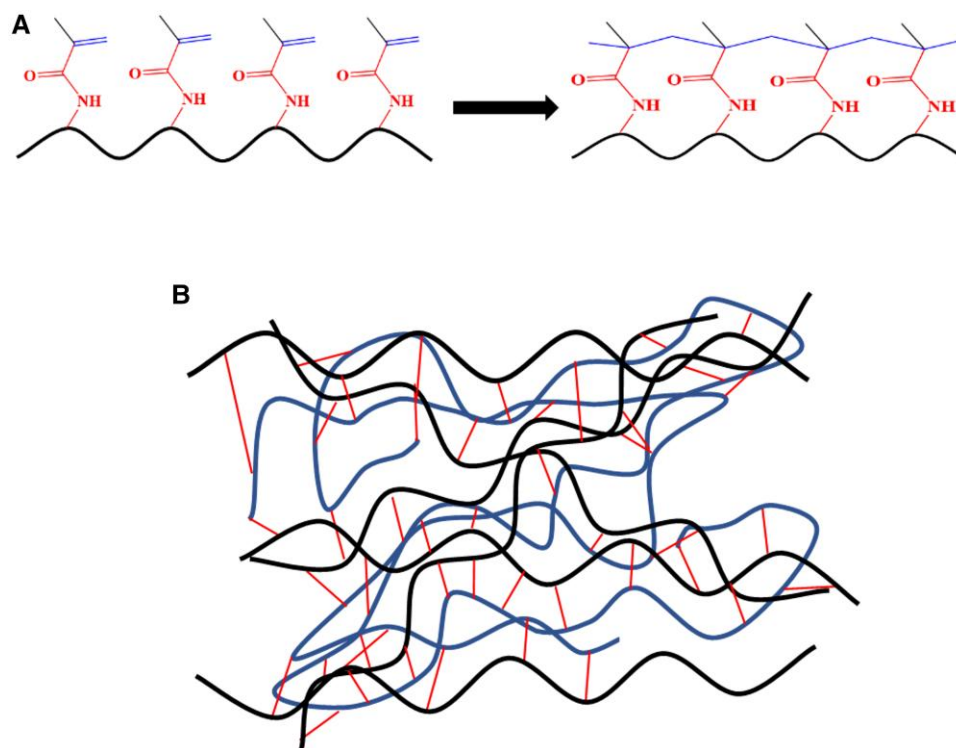
Erkoc et al. (96) applied a polymer-salt ATPS, gelatin/potassium phosphate ( $\text{K}_2\text{HPO}_4$ ), to generate hydrogel microspheres. They prepared three different mixtures, including 40, 20, and 15%  $\text{K}_2\text{HPO}_4$ , to study the effect of using an ATPS for hydrogel preparation. The results show that since the separated phases were more concentrated in their main compounds at higher  $\text{K}_2\text{HPO}_4$  amounts (40 and 20%), the gelatin phase exhibited high viscosity that led to larger aggregates. The ATPS with 15%  $\text{K}_2\text{HPO}_4$  led to the formation of submicron to nano-size aggregates. The resulting emulsion was crosslinked

utilizing two different methods, UV crosslinking of acrylates, and chemical crosslinking using *N*-(3-dimethylaminopropyl)-*N*'-ethylcarbodiimide hydrochloride (EDC) and *N*-hydroxysuccinimide (NHS). For UV crosslinking, a prepolymer aqueous solution of methacrylic anhydride-conjugated gelatin, eosin Y, TEA, and 1-vinyl-2-pyrrolidinone was added slowly to  $\text{K}_2\text{HPO}_4$  solution, and the emulsion was exposed to UV. In order to chemically crosslink the hydrogel droplets, EDC and NHS were added to the fluorescein isothiocyanate (FITC)-gelatin/ $\text{K}_2\text{HPO}_4$  ATPS, and the results showed that both methods were capable of crosslinking the hydrogel microspheres.

### Ionic crosslinking

In the ionic crosslinking method, polymers in aqueous droplets obtained from ATPSs are crosslinked through ionic bonds most commonly using sodium alginate and  $\text{Ca}^{2+}$  ions (Scheme 2) for stabilization (119).

In such an approach, sodium alginate and  $\text{Ca}^{2+}$  were added in different phases. Abbasi et al. (97) fabricated pollen-like spiky microparticles using a PEG/dextran ATPS and ionic crosslinking of alginate with calcium chloride ( $\text{CaCl}_2$ ). Partitioning of alginate was studied in three mixture points with varied dextran concentrations, and the mixture point with the highest dextran concentration, which could partition alginate to the dextran phase more efficiently, was selected for droplet generation. The dispersed phase of dextran-alginate droplets was generated in a continuous PEG phase using a flow-focusing microfluidic device and exhibited a size range of 50–80  $\mu\text{m}$ . The droplets were flowed to a PEG- $\text{CaCl}_2$  bath to trigger ionic polymerization and spike formation. Due to



**Scheme 1.** Schematic representation of crosslinking of acrylate functional groups (A), which can result in a crosslinked polymeric network (B).

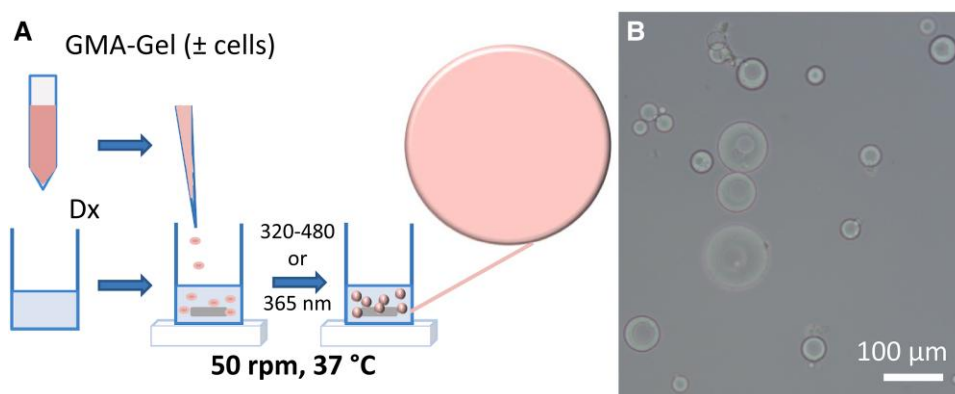


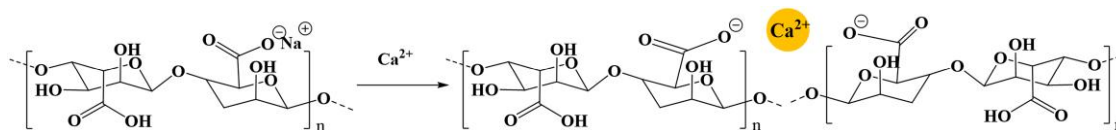
**Fig. 4.** A) GMA-gelatin microparticle preparation procedure. B) Optical microscopy image of the microparticle. Reproduced with permission from Ref. (94).

the concentration gradient across the PEG–dextran interface, CaCl<sub>2</sub> and water molecules diffused toward PEG in the continuous phase. This altered the equilibrium of dextran-alginate droplets, which resulted in alginate and dextran diffusion outward in the form of spikes. The dextran-alginate and CaCl<sub>2</sub> molecules initiated the ionic polymerization, which terminated the spike growth and the pollen-like spiky microparticles were fabricated. The presence of alginate both in the continuous phase and inside the droplets is necessary for spike formation. Higher PEG concentrations were found to reduce the length of spikes, due to the enhanced CaCl<sub>2</sub> gradient between the PEG–CaCl<sub>2</sub> bath and PEG phase, which accelerated both the CaCl<sub>2</sub> diffusion and dextran-alginate equilibrium disruption.

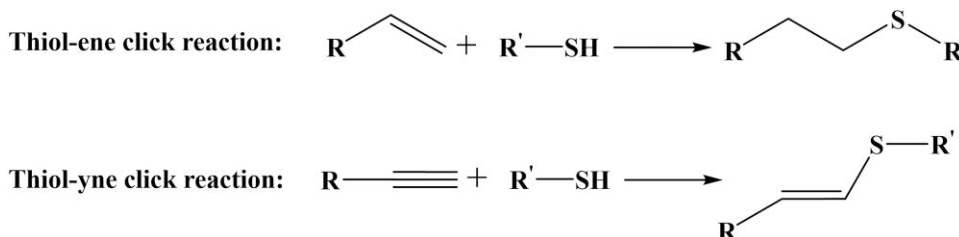
Alternately, sodium alginate and Ca<sup>2+</sup> ions can be added to the same phase simultaneously. Wang et al. (109) applied a microfluidic ATPS for the fabrication of multicompart ment hydrogel

capsules using ionic crosslinking. In order to generate dual-core capsules, two core flows containing a dextran phase, a shell flow of a PEG solution containing sodium alginate and calcium disodium ethylene diamine tetraacetate (Ca-EDTA), and a continuous phase flow of mineral oil containing acetic acid were introduced to the orifice of a flow-focusing microfluidic device. This formed droplets in the final laminar flow, released Ca<sup>2+</sup> ions from Ca-EDTA in the shell of the droplet due to the presence of acetic acid, and led to ionic crosslinking of sodium alginate. The size and morphology of the hydrogel capsules was controlled by adjusting the flow rates and acetic acid concentration, as well as utilizing chitosan as an additive.

Dumas et al. (111) applied a Pickering-like emulsion technique to stabilize the droplets of a dextran phase dispersed in a continuous PEG phase in a PEG/dextran ATPS. They added lipid nanocapsules (LNCs) or chitosan-grafted LNC (LNC-CS) to a specific mixture



**Scheme 2.** Ionic crosslinking using sodium alginate and calcium ion.



**Scheme 3.** The mechanisms of thiol-ene and thiol-yne click reactions.

point of the ATPS near the binodal curve, and used confocal microscopy to study the stability of dextran droplets over 28 days or through centrifugation or dilution. The ATPS (without additive) was separated into two phases by centrifugation: a dextran-rich phase at the bottom and PEG-rich phase on the top. Dilution moved the mixture point to the single-phase region of the phase diagram. The time stability study showed the coalescence of dextran droplets from day 7 onwards. The addition of LNC or LNC-CS to the ATPS led to the formation of clusters of LNC or the spread of LNC-CS around the droplets, respectively. Although LNC and LNC-CS were unable to stabilize the droplets over time and no pellets were observed after centrifugation, some small dextran droplets were formed after dilution of LNC-CS samples, demonstrating the potential of LNC-CS for stabilization of the droplets. Using the polyelectrolyte complexation ability of chitosan and alginate, a thick shell of LNC-CS was formed around the dextran droplets through ionic crosslinking (Fig. S3). The gelled ATPS-LNC-CS microparticles were stable over 28 days, and even after centrifugation or dilution of the droplets.

### Click reaction crosslinking

Click chemistry has also been used for crosslinking in ATPS droplets; this approach uses a stepwise growth route of polymerization, and a linker with high stability is formed between orthogonal compounds (120–122). The thiol-ene and thiol-yne click reactions (Scheme 3) are most commonly used to prepare microparticles from ATPS (123, 124).

Mytnyk et al. (113) used an ATPS to prepare microcapsules with an aqueous PEG-based core and a dextran-based hydrogel shell, using the thiol-yne click reaction for photocrosslinking. To prepare a stream of cross-linkable dextran, alkyne-functionalized dextran (dextran-glycidyl propargyl ether, dextran-GPE) and thiol-functionalized dextran (dextran-SH) were prepared and mixed. Four streams were fed to a microfluidic device: an aqueous PEG solution used as the core phase, two cross-linkable dextran solutions as the shell, and an outer PEG solution (Fig. 5A). The high concentration of PEG in the latter stream was selected to increase viscosity, preventing droplets from contacting the bottom of the channel and reducing fouling. For the click reaction between the thiol and alkyne groups (Fig. 5B), the droplets were irradiated at one of the channel bends to increase the UV-exposure time. The photoinitiator (Irgacure 2959) was added to all streams in equal concentrations to hinder its partitioning out of the cross-linkable phase.

Tae et al. (114) prepared  $\beta$ -glucan-incorporated PEG (PEG/SPG hybrid) microgels via a PEG/dextran ATPS and the thiol-ene photo-click reaction. They functionalized a four-arm-PEG and schizophyllan (SPG, a water-soluble  $\beta$ -glucan) to prepare four-arm-PEG-norbornene (PEG4NB) and SPG-norbornene (SPG-NB). A network structure was prepared utilizing thiyl radicals and the vinyl bonds of functional groups on PEG arms in the precursor solution via photopolymerization and UV exposure; the resulting material was subsequently added to the dextran solution. The mixture was emulsified using ultrasonication and then exposed to UV light. PEG microgels were formed and then incubated with functionalized SPG, followed by UV exposure. Figure S4A shows the presence of SPG (labeled by rhodamine B, red fluorescence) in the structure of 5(6)-carboxyfluorescein-labeled bovine serum albumin (FAM-BSA)-loaded microgels (green fluorescence). The size of PEG/SPG microgels was adjusted through concentration of the dextran phase. Further control over the particle size was obtained by optimizing the duration and power of ultrasonication. The effective incubation time for SPG incorporation in the microgel structure was investigated by measuring the surface charges of microgels and flow cytometry, which indicated that increasing incubation time did not increase SPG content. In addition, the negative surface charge and the fluorescence intensity of microgels were constant after incubation of the microgels with SPG at all incubation times (Fig. S4B and C).

### Phase-guided block copolymers assemblies

Self-assembly of amphiphilic block copolymers has been extensively studied for drug carrier preparation (122, 125, 126). Nanoparticles can be prepared from amphiphilic copolymers through solvent-free self-assembly (127, 128), solvent switching (129, 130), and emulsification (122, 125, 131). Depending on the hydrophilic fraction of the copolymer, various morphologies can be constructed, including micelles and bilayer vesicles. These methods encapsulate the desired cargo based on the volume fraction (105), which is low compared with the continuous phase, and do not provide the possibility of preparing asymmetrical structures. In addition, the need for organic solvents for particle formation, the application of postprocessing techniques, such as rotary evaporation, centrifugation, sonication, and filtration for solvent removal and size distribution control, can be time and energy intensive and difficult to scale (105, 116).

ATPSs have been considered as an alternative for polymersome and micelle preparation; assemblies are formed by the

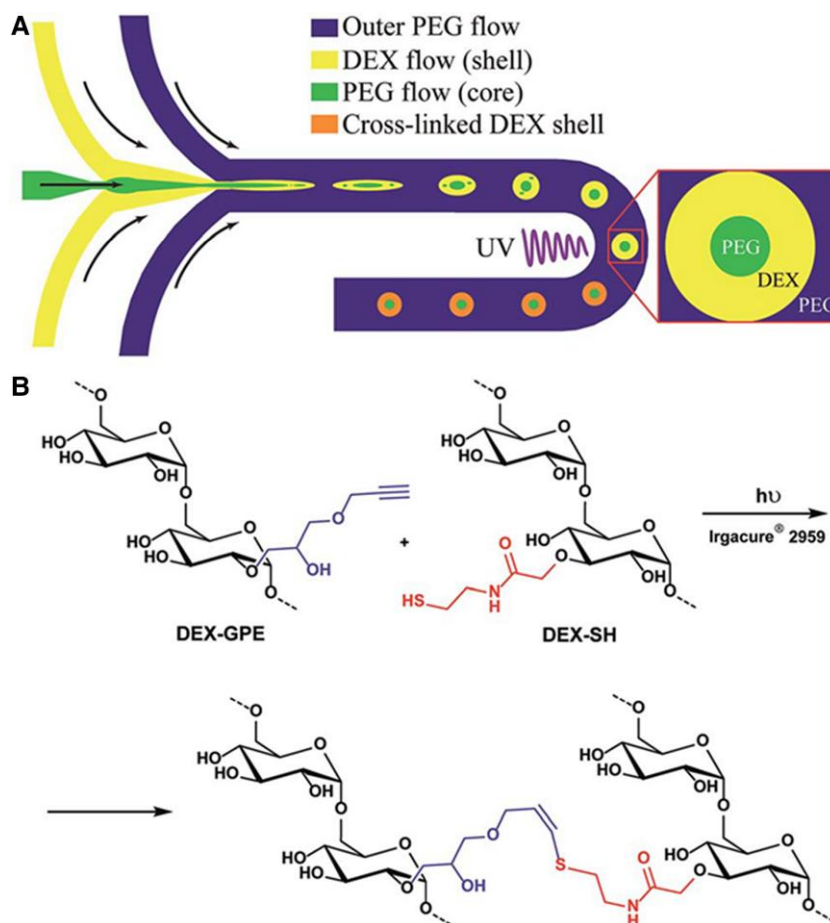


**Fig. 5.** A) Schematic representation of microfluidic device for PEG/dextran microcapsule preparation using ATPS. B) Thiol-yne click reaction and photocrosslinking of dextran phase. Reproduced with permission from Ref. (113).

aggregation of hydrophilic blocks of the copolymers around the ATPS droplets and the aggregation of hydrophobic blocks to decrease interactions with water. This leads to the formation of a core-shell structure with an aqueous core and a three-layered membrane. For example, a PEG/GMA-dextran ATPS has been applied to construct asymmetric polymersomes with different chemical properties in the inner and outer layers of the membrane (105). Employing ATPSs in asymmetric polymersome self-assembly leads to encapsulation of biomolecules based on thermodynamic partitioning.

Zhang et al. (105) added PEG-*b*-PCL and dextran-*b*-PCL diblock copolymers to a PEG/GMA-dextran ATPS. The dextran-*b*-PCL copolymers formed aggregates at the interface of the ATPS around droplets of the dextran dispersed phase. The PEG-*b*-PCL copolymers formed an outer leaflet such that the PEG blocks were in contact with PEG continuous phase (Fig. 6). The aqueous core, which was based on the GMA-dextran phase, was solidified through free radical initiated catalyzed methacrylate crosslinking. The asymmetry of the polymersomes was confirmed through confocal microscopy, as demonstrated by the diffusion of Nile red dye into the membrane of polymersome after bleaching. 2D-NOESY-NMR showed that no cross-peaks and spatial correlations between PEG and dextran blocks were formed.

Micellar carriers can be prepared from block copolymers using the same method as polymersome formation, provided the copolymers have smaller hydrophilic fractions. Kurnik et al. (116) prepared polymeric micelles from Pluronic L35, a triblock

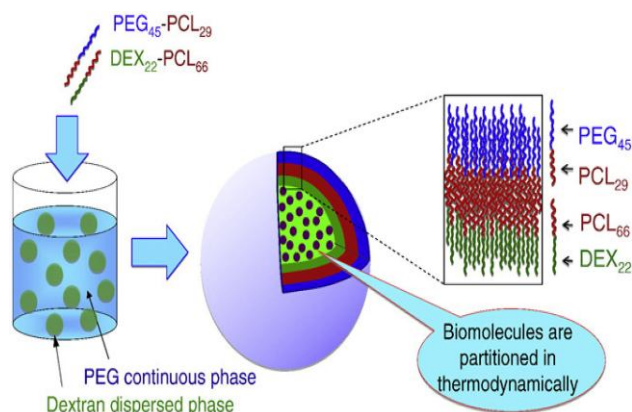


**Fig. 6.** The Preparation of asymmetric polymersomes using ATPSs. Reproduced with permission from Ref. (105).

copolymer with thermo-responsive behavior comprised of PEG and PPG (PEG<sub>11</sub>-PPG<sub>16</sub>-PEG<sub>11</sub>). Pluronic L35 is well-known to self-assemble into micelles during phase separation at concentrations higher than critical micelle concentration and at temperatures higher than lower critical solution temperature (LCST). The partitioning of curcumin as a model hydrophobic drug in an ATPS based on Pluronic L35 and various cholinium-based ionic liquids including cholinium hexanoate [Ch][Hex], cholinium butanoate [Ch][But], cholinium propanoate [Ch][Pro], cholinium acetate

[Ch][Ac], and cholinium chloride [Ch]Cl was studied. The hydrophobic drug partitioned into the polymer-rich phase, where it loaded into the micelles. The drug partitioning increased as the hydrophobicity of the ionic liquid increased. In addition, the hydrodynamic diameter of the micelles increased due to enhanced hydrophobic interactions between the PPG block and alkyl chain of the anion. The micelles were separated from the APTS using freeze drying, and their stability was studied at three temperatures over 30 days; the micelles remained colloidally stable at all temperatures for 30 days, but mean size increased at 37 °C relative to 4 and 25 °C.

## ATPS-based particles as drug carriers

Various microparticles and nanoparticles constructed using APTSs have been studied as carriers for drug delivery (87, 94–96, 98, 100, 102, 103, 105, 107–110, 114–116). Drug encapsulation is usually carried out by dissolving the cargo into the aqueous solution of one of the phase-forming compounds (105), direct addition to the APTS (110), or incubation of the obtained carriers with the cargo (107).

For example, encapsulation of drug-loaded liposomes into the hydrogel network of an APTS microparticle was reported to increase drug bioavailability at the target site (110). Preformed liposomes have been encapsulated into hydrogel microspheres of PEG/methacrylated-dextran APTSs via two routes: the addition of liposomes into the phase separated APTS or the addition of liposomes to the dextran feed solution. Liposomal encapsulation efficiencies of 88 and 94% were reported for the two approaches. After 17 days in pH 7.2 media, 10% of liposomes were released and were found to be in an intact form (110). The degradation of carbonate esters of crosslinked microspheres, which significantly increased after day 17, led to mesh size growth that in turn substantially increased liposome cumulative release.

Another study investigated protein encapsulation and stabilization potential using asymmetric bilayered polymersomes prepared in an APTS (105). Recombinant human erythropoietin was added to a dextran solution before APTS formation, and block copolymers were added to the APTS to form polymersomes, which were subsequently solidified. The encapsulation efficiency of erythropoietin into the asymmetric polymersomes was 89%, significantly higher than the protein encapsulation efficiency of the previously reported symmetric polymersomes (5%) (132), and protein bioactivity was preserved. This could be attributed to the chemically different interior medium of asymmetric polymersomes and the thermodynamic tendency of the protein to partition in the dextran phase, which formed the aqueous core of the polymersome.

Okur et al. (107) loaded doxorubicin into CREKA-functionalized microparticles prepared in the PEG/dextran APTS described in the section above on photopolymerization of acrylate functional groups. Loading was carried out by shaking the microparticles with an aqueous solution of the drug. The drug release profile in physiological pH was investigated, and a saturated cumulative release was obtained after 144 h. The doxorubicin-loaded CREKA-functionalized microparticles were found to internalize into HeLa cells more efficiently than free doxorubicin; the reported mechanism involved targeting of CREKA peptide to collagen IV in fibrin, which HeLa cells secrete as an extracellular protein (107).

The PEG/SPG hybrid microgels prepared via a PEG/dextran APTS and thiol-ene photo-click reaction (114) were loaded with BSA by adding BSA to the PEG4NB precursor solution prior to photopolymerization, and an 88% loading efficiency was reported. The microgels showed no cytotoxicity on RAW264.7 and NIH3T3

cells and were internalized only by the RAW264.7 cells (both naïve and lipopolysaccharide (LPS) activated; Fig. S5). Treating the RAW264.7 cells with LPS activates phagocytosis, by which the cells uptake the microgels. These macrophages can distinguish the SPG incorporated in microgels through their receptors, which leads to particle internalization. The release profile of BSA was investigated at pH 7.4 and 5. An initial burst release was observed in the first 24 h, and <15% of loaded BSA was released after 432 h. The slower release at pH 5 compared with pH 7.4 was attributed to the protonation of carboxylic groups in the SPG structure at pH 5, which slowed the BSA diffusion into the microgel network. FAM-BSA was shown to escape from the microgels internalized in RAW264.7 cells (114).

Simultaneous surface modification of SiO<sub>2</sub> nanoparticles and doxorubicin loading were reported using a PEG/lysine APTS (100). Since preferential partitioning of doxorubicin and SiO<sub>2</sub> toward the PEG phase was observed, the PEG-rich top phase was isolated and the resulting nanoformulations were used for subsequent drug release studies. The encapsulation efficiency of doxorubicin into SiO<sub>2</sub> nanoparticles increased significantly after SiO<sub>2</sub> surface modification. Encapsulation into nanoparticles slowed the release of doxorubicin at pH = 7.4 compared with free drug, with bare SiO<sub>2</sub> nanoparticles also showing a 16% higher cumulative release after 72 h compared with doxorubicin-loaded into surface-modified SiO<sub>2</sub> nanoparticles (Fig. 7) (100).

An area of growing interest is the encapsulation of live cells such as stem cells in carriers for applications in cell therapy (133). The sensitivity of cells to temperature, pH, and chemical species present in the environment limits the suitable methods for the preparation of cell-loaded carriers with controlled size. The preparation of water-in-oil emulsions (W/O) (134), water-oil-water emulsions (W/O/W) (135), and oil-in-water emulsions (O/W) (136) require surfactants (137), can introduce cells into direct contact with organic solvents, and need subsequent workup to remove any organic solvents. Therefore, there are limitations in using these emulsions for live cell encapsulation. APTS-based approaches are an attractive alternative for cell encapsulation in an all-aqueous system (87, 94, 103, 109). *Pseudomonas aeruginosa* bacteria were encapsulated in microcapsules prepared in a PEG/dextran APTS, which were surrounded by a polyelectrolyte-based shell (87). The bacteria were mixed along with nutrients in the dextran phase prior to microparticle formation. A live/dead assay (Fig. 8) indicated nutrients present in the microcapsules, and the permeability of the microcapsule shell enabled nutrient transport required for cell growth.

In another study, Wang et al. (109) prepared multiaqueous core hydrogel capsules using a microfluidic APTS with PEG and dextran as the shell- and core-forming phases, respectively. The shell was crosslinked using calcium alginate. These multicore hydrogel capsules were employed to encapsulate human liver cells (HepG2), which were suspended in one of the core flows (Fig. 9) during microparticle formation. The live/dead assay showed high cell viability (>95%) after 7 days of culture, representing the biocompatibility of the applied APTS process and the utilized polymers. Microparticle permeability enabled the movement of nutrients, oxygen, and metabolites that helped cells survive. As shown in Fig. 9, the multiaqueous core hydrogel capsules could encapsulate two different cell cultures, HepG2, and human umbilical vein endothelial cells (HUVECs), separately in their compartments (109).

## Stimuli-responsive APTS-based carriers

In addition to loading the drug into the carrier with high efficiency, it is essential to deliver the cargo to relevant pathological site and

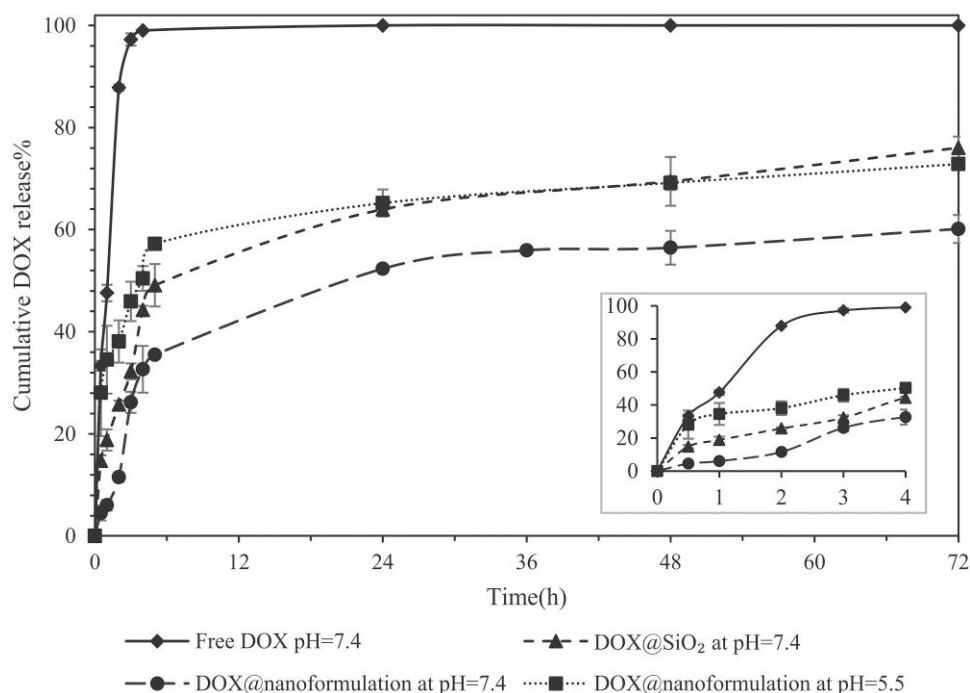


Fig. 7. Doxorubicin release profile from surface-modified SiO<sub>2</sub> nanoparticles. Reproduced with permission from Ref. (100).

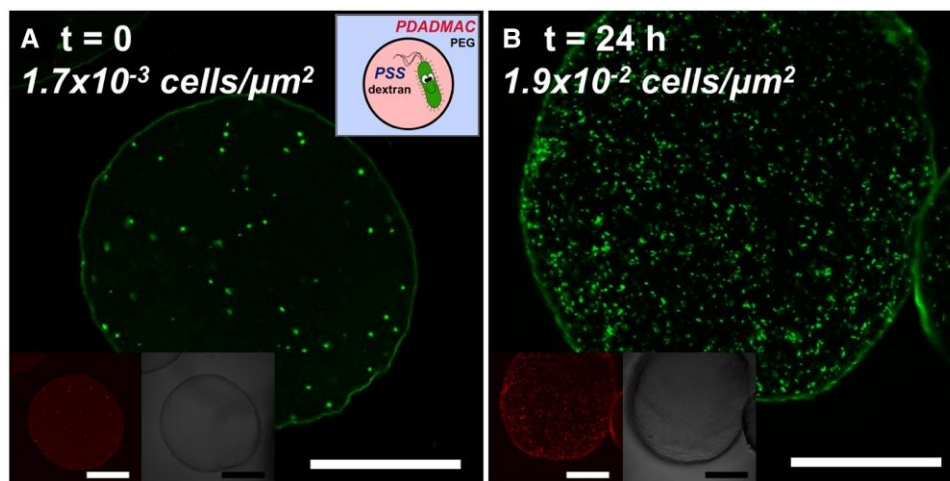


Fig. 8. Confocal microscopic images of *P. aeruginosa*-loaded microcapsules with a polyelectrolyte-based shell, analyzed through live/dead assay. Cells were stained with SYTO 9 (all cells) and propidium iodide (dead cells). A)  $t = 0$  h, B)  $t = 24$  h. All scale bars = 100  $\mu\text{m}$ . Reproduced with permission from Ref. (87).

release it at the target site (138–140). This can be addressed by developing stimuli-sensitive carriers that, in the presence of an appropriate stimulus, undergo changes in their shape, structure, or chemical properties (122). To prepare stimuli-sensitive carriers, a precise understanding of the target's biological environment is of particular importance. The stimuli used in the design of these carriers are divided into two major categories: endogenous and exogenous. Endogenous stimuli include redox, pH, enzyme, ionic strength, and glucose, which are based on the intrinsic conditions of the target site and act based on the difference in the pathological properties of diseased and healthy tissue. Endogenous stimuli are advantageous due to their self-controlled drug release from carriers and facile clinical application (138, 139, 141, 142). Exogenous stimuli, such as temperature, light, ultrasound,

magnetic fields, and electrical pulses, can be applied externally, and their advantages include the ability to accurately control the spatial and temporal release of the drug and the dose of the released drug (138, 139, 141). Various stimuli-responsive carriers prepared using ATPSS are summarized in Table 2.

## pH

pH is one of the most common stimuli utilized in drug delivery (100, 143–145), as pH varies by organ and organelle. For example, the pH range in the endosome and lysosome are 5–6.5 and 4.5–5, respectively, while the physiological pH is 7.4. The pH range in cancerous tissue is 6.5–7.2, due to the application of aerobic and anaerobic glycolysis metabolism in cancerous cells (138, 141,

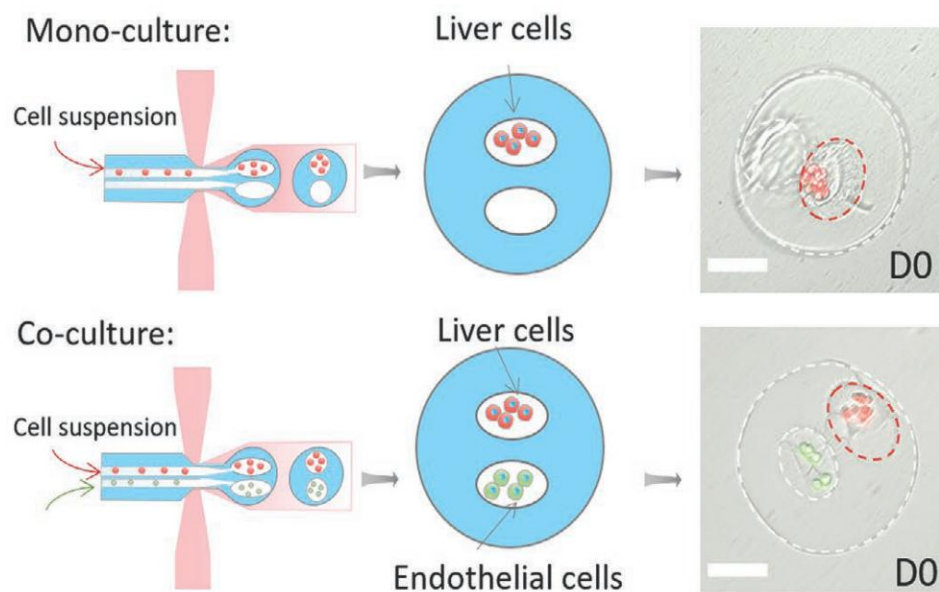


**Fig. 9.** Schematic representation and overlay images of HepG2-loaded multiaqueous core hydrogel capsules with/without HUVECs at day 0. Reproduced with permission from (109).

146). This pH difference can be used to develop pH-sensitive drug delivery systems. SiO<sub>2</sub> nanoparticles surface-modified in an APTS using hydrogen bonding have been shown to exhibit pH-responsive behavior (100). As reported elsewhere (147, 148), hydrogen bonding responds to pH changes and can be broken in acidic pH. The hydrogen bonding between the silanol groups on the surface of SiO<sub>2</sub>, the ethereal and terminal OH groups of PEG, and phenolic and amine groups of doxorubicin were broken faster in acidic media, which resulted in increased drug release in comparison with physiological pH (Fig. 7). Drug release in the presence of 10% fetal bovine serum at pH 7.4 versus 5.5 indicated that the presence of proteins in the medium could slightly slow down the drug release rate. This effect was more evident at acidic medium where the hydrogen bonds were broken and in the absence of the stealth property of PEG, the interactions between nanoparticles' surface and proteins increased and the formed protein corona affected the drug release profile (100).

## Temperature

Temperature-responsive drug delivery has been widely investigated (149–151), and a common method for preparing such carriers is utilizing polymers with an LCST near to physiological temperature 37 °C. Above the LCST, the polymer becomes insoluble, which can be used for drug release. Adjusting the nature and composition of the polymer is crucial for drug release at the target site, so that its LCST is higher than the body's temperature (139, 146). As previously discussed, Pluronic F127/PLGA microparticles (95) exhibited temperature-responsive behavior due to the presence of PPG in the copolymer structure. As temperature increases, the solubility of PPG decreases, leading to faster phase separation at lower concentrations. This results in smaller microparticles (Fig. S6). Studying the effect of temperature on cargo release showed an elevated drug release at 37 °C, which is in the range of LCST of PPG, compared with room temperature and 4 °C. This temperature facilitated phase separation, which caused the Pluronic F127 to shrink and expel water and water-dissolved compounds from the carrier. Similar results were obtained for

drug release from curcumin-loaded Pluronic L35 micelles prepared in an APTS (116). At temperatures below the LCST, the hydrophobic drug (curcumin) was stabilized in the hydrophobic core of the micelle and cannot diffuse through the corona. However, the hydrophobicity of the corona increased at temperatures higher than LCST, which facilitated drug diffusion from the hydrophobic corona and its adjacent aqueous media.

## Ultrasound

Ultrasound is a noninvasive exogenous stimulus with good penetrating power into tissue, and its thermal or mechanical effects can cause drug release. For example, cavitation caused by ultrasonic irradiation can destabilize carriers and trigger drug release (141, 146). For instance, Field et al. (98) prepared core-shell microparticles with a dextran-based core and PEGDA as the shell (Fig. S7). They actuated the microparticles using focused ultrasound, which caused cavitation due to the formation, oscillation, and collapse of bubbles. This internal cavitation ruptured microparticles (Fig. S7A and B), resulting in elevated drug release (Fig. S7C and D).

## Ionic strength

In vivo ionic strength and osmotic pressure gradients have also been investigated for stimulus-sensitive drug delivery using polyelectrolytes (152–154). Carriers based on these polymers swell in an environment with low ionic strength due to repulsion between charged groups. In an environment with high ionic strength, ion exchange occurs with the medium, the charge of the carrier is neutralized, and relatively less expansion occurs. By increasing the ionic strength to high levels, the osmotic pressure gradient between the carrier and the environment leads to carrier shrinkage (142, 155). Hann et al. (87) prepared ionic strength/osmotic pressure-responsive microcapsules using poly(diallyl dimethylammonium chloride) (PDADMAC) and poly(sodium 4-styrene sulfonate) (PSS) polyelectrolytes in a PEG/dextran APTS. The microcapsules comprised dextran droplets in the outer PEG phase, and the polyelectrolytes formed complexes at the droplet interface. As shown in Fig. S8A and B, by changing the PSS:PDADMAC

**Table 2.** Reported stimuli-responsive drug carriers prepared in ATPS.

Stimulus/targeting agent	Carrier	Cargo	Reference
pH Temperature	Surface-modified SiO <sub>2</sub> nanoparticles in a PEG/lysine ATPS	Doxorubicin	100 95, 116
	Pluronic F127/PLGA microparticles in a Pluronic F127/dextran ATPS Micelles based on Pluronic L35 in a Pluronic L35/ionic liquid ATPS	Rhodamine B, Coumarin-6 Curcumin	
Ultrasound Ionic strength and osmotic pressure change CREKA peptide	Core-shell microparticles based on a dextran/PEGDA ATPS	FITC-dextran	98
	Microcapsules based on a PEG/dextran ATPS surrounded by a membrane based on polyelectrolytes	Rhodamine B-tagged dextran (RD70)	87
	CREKA-functionalized PEG nanoparticles prepared in a PEG/dextran ATPS	Doxorubicin	107

ratio from 0.07:1 to 4:1 and dialyzing the resulting microcapsules against pure water to subject them to negative osmotic pressure, the permeability of the microcapsules changed and they lost their integrity, which led to release of rhodamine B-tagged dextran (RD70). Additionally, changing the ionic strength of the solution at a higher concentration of NaCl led to a significant size shrinkage of the microcapsules due to the altered permeability of the shell, which led to increased cargo release (Fig. S8C and D).

The drug delivery systems reviewed so far have been based on passive targeting, in which the drug is released based on the pathological conditions at the target site. Another option is active targeting, in which ligands such as peptides, aptamers, antibodies, etc. are embedded in the carrier structure (138, 139, 156). Active targeting can significantly improve carrier internalization into the cell. CREKA peptide is a tumor-homing peptide that has been applied for targeting tumor blood vessels (107). The targeting ability of the CREKA-functionalized microparticles prepared using the PEG/dextran ATPS was studied through binding affinity investigations (107). CREKA shows a specific affinity toward fibrin, a tough protein involved in blood clotting. The fibrin-binding ratio of free CREKA, nanoparticles without CREKA, and CREKA-conjugated nanoparticles were 70, 45, and 94%, respectively. This shows that functionalizing the carrier using targeting agents can increase the accumulation of the particles at the desired tumor site.

## Conclusion and future prospects

ATPSs have gained attention in diverse applications, including separation and purification processes, and more recently, as carriers for drug delivery. Their appeal lies in their facile constructability, cost-effectiveness, scalability, and compatibility with biological and pharmaceutical compounds within a biocompatible aqueous environment. Prudent selection of phase-forming compounds and precise control of mixing conditions are critical to customizing ATPS characteristics to suit specific requirements. Of particular note is how broadly the approach can be applied in drug delivery: the ATPS approach has been used to load a broad range of bioactive materials, including small molecule hydrophobic drugs, small molecule hydrophilic drug, proteins, and even intact cells. The possibility for co-loading multiple compounds from different chemical classes for therapeutic synergy and encapsulating nucleic acids which are rapidly being developed for therapeutic applications is an attractive prospect as the field continues to develop.

In the context of ATPS-based particle formation, several methodologies have been devised to fabricate micro- and nanoparticles, utilizing the unique properties inherent to ATPSs.

1. ATPS-guided particle formation involves introducing a compound into an ATPS, leading to its preferential partitioning

into one phase and initiating particle formation through intercomponent interactions.

2. Polymerization of droplets in ATPSs utilizes processes, such as photopolymerization of acrylate functional groups and ionic crosslinking within distinct ATPS droplets, resulting in the production of polymer-based particles.
3. Phase-guided block copolymer assembly leverages hydrophilic/hydrophobic interactions between amphiphilic block copolymers present in an ATPS, facilitating the assembly of particles with predetermined structural characteristics that are otherwise difficult to produce.

Multiple routes exist for loading pharmaceutical compounds into these carriers: dissolving the cargo into the aqueous solution of phase-forming compounds, direct addition to the ATPS, or incubation of carriers with the cargo. This flexibility enables loading of payloads with a broad range of physical chemistries highlighted above. Additionally, stimuli responsiveness can be introduced into ATPS-based carrier structures through responsive linkers or polymers, which enables the development of particles responsive to diverse endogenous and exogenous stimuli. ATPS-based carriers with active targeting ligands have also been engineered.

There are still unmet challenges that persist in the use of ATPSs for drug delivery applications, and these should be the focus of future work in the field. These include processing issues, e.g. efficient retrieval of formed particles, particularly in dilute systems, and scale-up beyond the used microfluidic mixers. Additionally, the overall lack of in vivo data in the literature limits the extent to which common biological mechanisms can be determined and generalized to streamline formulation development and clinical translation.

## Supplementary Material

Supplementary material is available at PNAS Nexus online.

## Funding

No funding was received for the preparation of this article.

## Author Contributions

**M.B.:** conceptualization, investigation, writing—original draft. **H.S.S.:** investigation, writing—original draft. **A.K. and K.R.:** supervision, writing—review and editing. **G.P.:** conceptualization, supervision, writing—review and editing.

## References

1. Yau YK, et al. 2015. Current applications of different type of aqueous two-phase systems. *Bioresour Bioprocess.* 2:49.

- 2 Raja S, Murty VR, Thivaharan V, Rajasekar V, Ramesh V. 2011. Aqueous two phase systems for the recovery of biomolecules—a review. *Sci Technol*. 1:7–16.
- 3 Torres-Acosta MA, Mayolo-Deloya K, González-Valdez J, Rito-Palomares M. 2019. Aqueous two-phase systems at large scale: challenges and opportunities. *Biotechnol J*. 14:1800117.
- 4 Chao Y, Shum HC. 2020. Emerging aqueous two-phase systems: from fundamentals of interfaces to biomedical applications. *Chem Soc Rev*. 49:114–142.
- 5 Varadavenkatesan T, Pai S, Vinayagam R, Pugazhendhi A, Selvaraj R. 2021. Recovery of value-added products from wastewater using aqueous two-phase systems—a review. *Sci Total Environ*. 778:146293.
- 6 Teixeira AG, et al. 2018. Emerging biotechnology applications of aqueous two-phase systems. *Adv Healthc Mater*. 7:1701036.
- 7 Iqbal M, et al. 2016. Aqueous two-phase system (ATPS): an overview and advances in its applications. *Biol Proced*. 181(18):1–18.
- 8 Asenjo JA, Andrews BA. 2012. Aqueous two-phase systems for protein separation: phase separation and applications. *J Chromatogr A*. 1238:1–10.
- 9 Phong WN, Show PL, Chow YH, Ling TC. 2018. Recovery of biotechnological products using aqueous two phase systems. *J Biosci Bioeng*. 126:273–281.
- 10 Ruiz-Ruiz F, Benavides J, Aguilar O, Rito-Palomares M. 2012. Aqueous two-phase affinity partitioning systems: current applications and trends. *J Chromatogr A*. 1244:1–13.
- 11 Oke EA, Ijardar SP. 2021. Insights into the separation of metals, dyes and pesticides using ionic liquid based aqueous biphasic systems. *J Mol Liq*. 334:116027.
- 12 Fick C, Khan Z, Srivastava S. 2023. Interfacial stabilization of aqueous two-phase systems: a review. *Mater Adv*. 4:4665–4678.
- 13 Sintra TE, et al. 2021. Sequential recovery of C-phycoerythrin and chlorophylls from *Anabaena cylindrica*. *Sep Purif Technol*. 255:117538.
- 14 Madeira PP, Reis CA, Rodrigues AE, Mikheeva LM, Zaslavsky BY. 2010. Solvent properties governing solute partitioning in polymer/polymer aqueous two-phase systems: nonionic compounds. *J Phys Chem B*. 114:457–462.
- 15 Madeira PP, et al. 2012. Salt effects on solvent features of coexisting phases in aqueous polymer/polymer two-phase systems. *J Chromatogr A*. 1229:38–47.
- 16 Nisslein M, González-González M, Rito-Palomares M. 2021. Influence of the line length and volume ratio on the partition behavior of peripheral blood and conjugated CD34 antibody in polymer-polymer aqueous two-phase systems. *Sep Purif Technol*. 257:117830.
- 17 Jue E, Yamanishi CD, Chiu RYT, Wu BM, Kamei DT. 2014. Using an aqueous two-phase polymer-salt system to rapidly concentrate viruses for improving the detection limit of the lateral-flow immunoassay. *Biotechnol Bioeng*. 111:2499–2507.
- 18 Wyszczanska K, Do HT, Held C, Sadowski G, Macedo EA. 2018. Effect of different organic salts on amino acids partition behaviour in PEG-salt ATPS. *Fluid Phase Equilib*. 456:84–91.
- 19 Chow YH, et al. 2015. Characterization of bovine serum albumin partitioning behaviors in polymer-salt aqueous two-phase systems. *J Biosci Bioeng*. 120:85–90.
- 20 Shaker Shiran H, Baghbanbashi M, Ahsaie FG, Pazuki G. 2020. Study of curcumin partitioning in polymer-salt aqueous two phase systems. *J Mol Liq*. 303:112629.
- 21 Ng HS, et al. 2021. Characterization of alcohol/salt aqueous two-phase system for optimal separation of gallic acids. *J Biosci Bioeng*. 131:537–542.
- 22 Lin YK, et al. 2013. Recovery of human interferon alpha-2b from recombinant *Escherichia coli* using alcohol/salt-based aqueous two-phase systems. *Sep Purif Technol*. 120:362–366.
- 23 Li F, Li Q, Wu S, Sun D, Tan Z. 2018. Salting-out extraction of sinomenine from *Sinomenium acutum* by an alcohol/salt aqueous two-phase system using ionic liquids as additives. *J Chem Technol Biotechnol*. 93:1925–1930.
- 24 Wang Y, Wang S, Liu L. 2021. Extraction of geniposidic acid and aucubin employing aqueous two-phase systems comprising ionic liquids and salts. *Microchem J*. 169:106592.
- 25 Gómez E, Requejo PF, Tojo E, Macedo EA. 2019. Recovery of flavonoids using novel biodegradable choline amino acids ionic liquids based ATPS. *Fluid Phase Equilib*. 493:1–9.
- 26 Wu X, Liu Y, Zhao Y, Cheong KL. 2018. Effect of salt type and alkyl chain length on the binodal curve of an aqueous two-phase system composed of imidazolium ionic liquids. *J Chem Eng Data*. 63:3297–3304.
- 27 Yu X, et al. 2021. Switchable (pH driven) aqueous two-phase systems formed by deep eutectic solvents as integrated platforms for production-separation 5-HMF. *J Mol Liq*. 325:115158.
- 28 Tu S, et al. 2022. Exploration of lower critical solution temperature DES in a thermoreversible aqueous two-phase system for integrating glucose conversion and 5-HMF separation. *Renew Energy*. 189:392–401.
- 29 Li N, et al. 2016. Development of green betaine-based deep eutectic solvent aqueous two-phase system for the extraction of protein. *Talanta*. 152:23–32.
- 30 Deng WW, Zong Y, Xiao YX. 2017. Hexafluoroisopropanol-based deep eutectic solvent/salt aqueous two-phase systems for extraction of Anthraquinones from *Rhei Radix et Rhizoma* samples. *ACS Sustain Chem Eng*. 5:4267–4275.
- 31 Liu Y, Wu Z, Dai J. 2012. Phase equilibrium and protein partitioning in aqueous micellar two-phase system composed of surfactant and polymer. *Fluid Phase Equilib*. 320:60–64.
- 32 Chávez-Castilla LR, Aguilar O. 2016. An integrated process for the in situ recovery of prodigiosin using micellar ATPS from a culture of *Serratia marcescens*. *J Chem Technol Biotechnol*. 91:2896–2903.
- 33 Mashayekhi F, Le AM, Nafisi PM, Wu BM, Kamei DT. 2012. Enhancing the lateral-flow immunoassay for detection of proteins using an aqueous two-phase micellar system. *Anal Bioanal Chem*. 404:2057–2066.
- 34 Mashayekhi F, et al. 2010. Enhancing the lateral-flow immunoassay for viral detection using an aqueous two-phase micellar system. *Anal Bioanal Chem*. 398:2955–2961.
- 35 Becker JS, Thomas ORT, Franzreb M. 2009. Protein separation with magnetic adsorbents in micellar aqueous two-phase systems. *Sep Purif Technol*. 65:46–53.
- 36 Ahsaie FG, Pazuki G, Sintra TE, Carvalho P, Ventura SPM. 2021. Study of the partition of sodium diclofenac and norfloxacin in aqueous two-phase systems based on copolymers and dextran. *Fluid Phase Equilib*. 530:112868.
- 37 Wang Y, Yang T, Zeng H, Wan J, Cao X. 2021. Study of lincomycin partition in a recyclable thermo-pH responsive aqueous two-phase system. *Process Biochem*. 109:27–36.
- 38 Zakrzewska ME, et al. 2021. Extraction of antibiotics using aqueous two-phase systems based on ethyl lactate and thiosulphate salts. *Fluid Phase Equilib*. 539:113022.
- 39 Jafari P, Jouyban A. 2021. Partitioning behavior of caffeine, lamotrigine, clonazepam and oxcarbazepine in a biodegradable aqueous two-phase system comprising of polyethylene glycol dimethyl ether 250 and choline chloride/saccharose deep eutectic solvent. *J Mol Liq*. 323:115055.
- 40 Kurnik IS, et al. 2020. Separation and purification of curcumin using novel aqueous two-phase micellar systems composed of

- amphiphilic copolymer and cholinium ionic liquids. *Sep Purif Technol.* 250:117262.
- 41 Velho P, Oliveira I, Gómez E, MacEdo EA. 2021. pH study and partition of riboflavin in an ethyl lactate-based aqueous two-phase system with sodium citrate. *J Chem Eng Data.* 67:1985–1993.
- 42 Berton P, Monasterio RP, Wuilloud RG. 2012. Selective extraction and determination of vitamin B12 in urine by ionic liquid-based aqueous two-phase system prior to high-performance liquid chromatography. *Talanta.* 97:521–526.
- 43 Veloso AV, et al. 2020. Selective and continuous recovery of ascorbic acid and vanillin from commercial diet pudding waste using an aqueous two-phase system. *Food Bioprod Process.* 119:268–276.
- 44 Wysoczanska K, Do HT, Sadowski G, Macedo EA, Held C. 2020. Partitioning of water-soluble vitamins in biodegradable aqueous two-phase systems: electrolyte perturbed-chain statistical associating fluid theory predictions and experimental validation. *AIChE J.* 66:e16984.
- 45 Chen J, Wang Y, Zeng Q, Ding X, Huang Y. 2014. Partition of proteins with extraction in aqueous two-phase system by hydroxyl ammonium-based ionic liquid. *Anal Methods.* 6:4067–4076.
- 46 Desai RK, Streefland M, Wijffels RH, Eppink MHM. 2014. Extraction and stability of selected proteins in ionic liquid based aqueous two phase systems. *Green Chem.* 16:2670–2679.
- 47 Li Z, Liu X, Pei Y, Wang J, He M. 2012. Design of environmentally friendly ionic liquid aqueous two-phase systems for the efficient and high activity extraction of proteins. *Green Chem.* 14:2941–2950.
- 48 Lin X, Wang Y, Zeng Q, Ding X, Chen J. 2013. Extraction and separation of proteins by ionic liquid aqueous two-phase system. *Analyst.* 138:6445–6453.
- 49 Campos-García VR, Benavides J, González-Valdez J. 2021. Reactive aqueous two-phase systems for the production and purification of PEGylated proteins. *Electron J Biotechnol.* 54:60–68.
- 50 Pérez MT, Pinilla M, Sancho P. 1999. In vivo survival of selected murine carrier red blood cells after separation by density gradients or aqueous polymer two-phase systems. *Life Sci.* 64:2273–2283.
- 51 Li M, Li D, Song Y, Li D. 2022. Tunable particle/cell separation across aqueous two-phase system interface by electric pulse in microfluidics. *J Colloid Interface Sci.* 612:23–34.
- 52 Edahiro JI, et al. 2005. Separation of cultured strawberry cells producing anthocyanins in aqueous two-phase system. *J Biosci Bioeng.* 100:449–454.
- 53 Goubbran Botros H, Birkenmeier G, Otto A, Kopperschlager G, Vijayalakshmi MA. 1991. Immobilized metal ion affinity partitioning of cells in aqueous two-phase systems: erythrocytes as a model. *Biochim Biophys Acta Gen Subj.* 1074:69–73.
- 54 Skuse DR, Norris-Jones R, Yalpani M, Brooks DE. 1992. Hydroxypropyl cellulose/poly(ethylene glycol)-co-poly(propylene glycol) aqueous two-phase systems: system characterization and partition of cells and proteins. *Enzyme Microb Technol.* 14:785–790.
- 55 Pavlovic M, et al. 2020. Cascade kinetics in an enzyme-loaded aqueous two-phase system. *Langmuir.* 36:1401–1408.
- 56 Souza RL, Ventura SPM, Soares CMF, Coutinho JAP, Lima AS. 2015. Lipase purification using ionic liquids as adjuvants in aqueous two-phase systems. *Green Chem.* 17:3026–3034.
- 57 Ventura SPM, et al. 2012. Production and purification of an extracellular lipolytic enzyme using ionic liquid-based aqueous two-phase systems. *Green Chem.* 14:734–740.
- 58 Matias da Silva Batista J, et al. 2021. Biotechnological purification of a  $\beta$ -fructofuranosidase ( $\beta$ -FFase) from *Aspergillus tamarii* kita: aqueous two-phase system (PEG/Citrate) and biochemical characterization. *Biocatal Agric Biotechnol.* 35:102070.
- 59 Jiang B, et al. 2021. Effective separation of prolyl endopeptidase from *Aspergillus Niger* by aqueous two phase system and its characterization and application. *Int J Biol Macromol.* 169:384–395.
- 60 Tang MSY, et al. 2014. Separation of single-walled carbon nanotubes using aqueous two-phase system. *Sep Purif Technol.* 125:136–141.
- 61 Ao G, Khripin CY, Zheng M. 2014. DNA-controlled partition of carbon nanotubes in polymer aqueous two-phase systems. *J Am Chem Soc.* 136:10383–10392.
- 62 Fagan JA. 2019. Aqueous two-polymer phase extraction of single-wall carbon nanotubes using surfactants. *Nanoscale Adv.* 1:3307–3324.
- 63 Subbaiyan NK, et al. 2014. Bench-top aqueous two-phase extraction of isolated individual single-walled carbon nanotubes. *Nano Res.* 85(8):1755–1769.
- 64 Milevskiy NA, Boryagina IV, Karpukhina EA, Kuznetsov VN, Kabanova EG. 2021. Effect of sodium chloride and pH on the composition of the equilibrium phases and the partition of palladium(II) in the aqueous two-phase system PEG1500-Na2SO4-water. *J Chem Eng Data.* 66:1021–1031.
- 65 Vargas SJR, Quintão JC, Ferreira GMD, Da Silva LHM, Hespanhol MC. 2019. Lanthanum and cerium separation using an aqueous two-phase system with ionic liquid. *J Chem Eng Data.* 64:4239–4246.
- 66 Muruchi L, et al. 2019. Sustainable extraction and separation of rhenium and molybdenum from model copper mining effluents using a polymeric aqueous two-phase system. *ACS Sustain Chem Eng.* 7:1778–1785.
- 67 Sun P, Huang K, Song W, Gao Z, Liu H. 2018. Separation of rare earths from the transition metals using a novel ionic-liquid-based aqueous two-phase system: toward green and efficient recycling of rare earths from the NdFeB magnets. *Ind Eng Chem Res.* 57:16934–16943.
- 68 da Silveira Leite D, et al. 2021. Selective recovery of zinc from mining sulfuric liquor employing aqueous two-phase systems. *J Water Process Eng.* 42:102138.
- 69 Huang Y, et al. 2021. A green method for recovery of thallium and uranium from wastewater using polyethylene glycol and ammonium sulfate based on aqueous two-phase system. *J Clean Prod.* 297:126452.
- 70 Chairez-Cantu K, González-González M, Rito-Palomares M. 2021. Novel approach for neuronal stem cell differentiation using aqueous two-phase systems in 3D cultures. *J Chem Technol Biotechnol.* 96:8–13.
- 71 Tavana H, Takayama S. 2011. Aqueous biphasic microprinting approach to tissue engineering. *Biomicrofluidics.* 5:13404.
- 72 Hao X, et al. 2022. Microfluidic particle reactors: from interface characteristics to cells and drugs related biomedical applications. *Adv Mater Interfaces.* 9:2102184.
- 73 Salamanca MH, Merchuk JC, Andrews BA, Asenjo JA. 1998. On the kinetics of phase separation in aqueous two-phase systems. *J Chromatogr B Biomed Sci Appl.* 711:319–329.
- 74 Johansson HO, Karlström G, Tjerneld F, Haynes CA. 1998. Driving forces for phase separation and partitioning in aqueous two-phase systems. *J Chromatogr B Biomed Sci Appl.* 711:3–17.
- 75 Walter H, Johansson G. *Aqueous two-phase systems, volume 228* Academic Press, San Diego, CA, 1994. p. 1–725.
- 76 Hatti-Kaul R. 2001. Aqueous two-phase systems: a general overview. *Mol Biotechnol.* 19:269–277.

- 77 Cláudio AFM, Ferreira AM, Shahriari S, Freire MG, Coutinho JAP. 2011. Critical assessment of the formation of ionic-liquid-based aqueous two-phase systems in acidic media. *J Phys Chem B*. 115: 11145–11153.
- 78 Tanimura K, et al. 2019. Characterization of ionic liquid aqueous two-phase systems: phase separation behaviors and the hydrophobicity index between the two phases. *J Phys Chem B*. 123: 5866–5874.
- 79 Hachem F, Andrews BA, Asenjo JA. 1996. Hydrophobic partitioning of proteins in aqueous two-phase systems. *Enzyme Microb Technol*. 19:507–517.
- 80 Grilo AL, Aires-Barros MR, Azevedo AM. 2016. Partitioning in aqueous two-phase systems: fundamentals, applications and trends. *Sep Purif Rev*. 45:68–80.
- 81 Forciniti D, Hall CK, Kula MR. 1991. Influence of polymer molecular weight and temperature on phase composition in aqueous two-phase systems. *Fluid Phase Equilib*. 61:243–262.
- 82 Glyk A, Scheper T, Beutel S. 2014. Influence of different phase-forming parameters on the phase diagram of several PEG-salt aqueous two-phase systems. *J Chem Eng Data*. 59:850–859.
- 83 Silvério SC, Rodríguez O, Teixeira JA, Macedo EA. 2013. The effect of salts on the liquid-liquid phase equilibria of PEG600 + salt aqueous two-phase systems. *J Chem Eng Data*. 58:3528–3535.
- 84 Ferreira LA, Teixeira JA. 2011. Salt effect on the aqueous two-phase system PEG 8000-sodium sulfate. *J Chem Eng Data*. 56: 133–137.
- 85 Hartounian H, Floeter E, Kaler EW, Sandler SI. 1993. Effect of temperature on the phase equilibrium of aqueous two-phase polymer systems. *AIChE J*. 39:1976–1984.
- 86 Waziri SM, Abu-Sharkh BF, Ali SA. 2003. The effect of pH and salt concentration on the coexistence curves of aqueous two-phase systems containing a pH responsive copolymer and polyethylene glycol. *Fluid Phase Equilib*. 205:275–290.
- 87 Hann SD, Niepa THR, Stebe KJ, Lee D. 2016. One-step generation of cell-encapsulating compartments via polyelectrolyte complexation in an aqueous two phase system. *ACS Appl Mater Interfaces*. 8:25603–25611.
- 88 Ahsaie FG, Pazuki G. 2021. Separation of phenyl acetic acid and 6-aminopenicillanic acid applying aqueous two-phase systems based on copolymers and salts. *Sci Rep*. 11(11):3489.
- 89 Domingues JT, et al. 2021. Extraction of estrogen hormones from water samples using an aqueous two-phase system: a new approach for sample preparation in the analysis of emerging contaminants. *Microchem J*. 166:106231.
- 90 Cohen Stuart MA, et al. 2010. Emerging applications of stimuli-responsive polymer materials. *Nat Mater*. 9:101–113.
- 91 Doméjean H, et al. 2016. Controlled production of sub-millimeter liquid core hydrogel capsules for parallelized 3D cell culture. *Lab Chip*. 17:110–119.
- 92 Lee SS, Abbaspourrad A, Kim SH. 2014. Nonspherical double emulsions with multiple distinct cores enveloped by ultrathin shells. *ACS Appl Mater Interfaces*. 6:1294–1300.
- 93 Watanabe T, Motohiro I, Ono T. 2019. Microfluidic formation of hydrogel microcapsules with a single aqueous core by spontaneous cross-linking in aqueous two-phase system droplets. *Langmuir*. 35:2358–2367.
- 94 Neffe AT, Garcia Cruz DM, Roch T, Lendlein A. 2021. Microparticles from glycidylmethacrylated gelatin as cell carriers prepared in an aqueous two-phase system. *Eur Polym J*. 142:110148.
- 95 Yeredla N, Kojima T, Yang Y, Takayama S, Kanapathipillai M. 2016. Aqueous two phase system assisted self-assembled PLGA microparticles. *Sci Rep*. 6(6):27736.
- 96 Erkok P, Dogan NO, Kizilel S. 2019. Optimization of a gelatin-potassium phosphate aqueous two-phase system for the preparation of hydrogel microspheres. *JOM*. 71(4):1264–1270.
- 97 Abbasi N, Navi M, Nunes JK, Tsai SSH. 2019. Controlled generation of spiky microparticles by ionic cross-linking within an aqueous two-phase system. *Soft Matter*. 15:3301–3306.
- 98 Field RD, et al. 2022. Ultrasound-responsive aqueous two-phase microcapsules for on-demand drug release. *Angew Chemie Int Ed*. 61:e202116515.
- 99 Liu Y, Zhu C, Fu T, Gao X, Ma Y. 2024. Breakup dynamics of water-in-water droplet generation in a flow-focusing microchannel. *Chem Eng Sci*. 283:119384.
- 100 Baghbanbashi M, Pazuki G, Khoee S. 2022. One pot silica nanoparticle modification and doxorubicin encapsulation as pH-responsive nanocarriers, applying PEG/lysine aqueous two phase system. *J Mol Liq*. 349:118472.
- 101 Gao Y, et al. 2023. Ability of soy protein derived amyloid fibrils to stabilize aqueous two-phase system and effect of pH on the system. *Food Hydrocoll*. 145:109084.
- 102 Harling S, Schwoerer A, Scheibe K, Daniels R, Menzel H. 2010. A new hydrogel drug delivery system based on hydroxyethylstarch derivatives. *J Microencapsul*. 27:400–408.
- 103 Liu Q, et al. 2019. Self-orienting hydrogel micro-buckets as novel cell carriers. *Angew Chemie Int Ed*. 58:547–551.
- 104 Ben Messaoud G, et al. 2024. Structuring gelatin methacryloyl-dextran hydrogels and microgels under shear. *Soft Matter*. 20: 773–787.
- 105 Zhang Y, Wu F, Yuan W, Jin T. 2010. Polymersomes of asymmetric bilayer membrane formed by phase-guided assembly. *J Control Release*. 147:413–419.
- 106 Zhang Y, et al. 2024. Emerging delivery systems based on aqueous two-phase systems: a review. *Acta Pharm Sin B*. 14:110–132.
- 107 Okur AC, Erkok P, Kizilel S. 2016. Targeting cancer cells via tumor-homing peptide CREKA functional PEG nanoparticles. *Colloids Surfaces B Biointerfaces*. 147:191–200.
- 108 Ma S, et al. 2012. Fabrication of microgel particles with complex shape via selective polymerization of aqueous two-phase systems. *Small*. 8:2356–2360.
- 109 Wang H, et al. 2020. Flexible generation of multi-aqueous core hydrogel capsules using microfluidic aqueous two-phase system. *Adv Mater Technol*. 5:2000045.
- 110 Stenekes RJH, Loebis AE, Fernandes CM, Crommelin DJA, Hennink WE. 2000. Controlled release of liposomes from biodegradable dextran microspheres: a novel delivery concept. *Pharm Res*. 17(17):664–669.
- 111 Dumas F, Benoit JP, Saulnier P, Roger E. 2021. A new method to prepare microparticles based on an Aqueous Two-Phase System (ATPS), without organic solvents. *J Colloid Interface Sci*. 599:642–649.
- 112 Zhang Q, Chen J, Gai H. 2019. High-throughput-generating water-in-water droplet for monodisperse biocompatible particle synthesis. *J Mater Sci*. 54(24):14905–14913.
- 113 Mytnyk S, et al. 2017. Microcapsules with a permeable hydrogel shell and an aqueous core continuously produced in a 3D microdevice by all-aqueous microfluidics. *RSC Adv*. 7: 11331–11337.
- 114 Tae H, Lee S, Ki CS. 2019.  $\beta$ -Glucan hybridized poly(ethylene glycol) microgels for macrophage-targeted protein delivery. *J Ind Eng Chem*. 75:69–76.
- 115 Ge X, et al. 2014. PEG-PCL-DEX polymersome-protamine vector as an efficient gene delivery system via PEG-guided self-assembly. *Nanomedicine (Lond)*. 9:1193–1207.

- 116 Kurnik IS, et al. 2021. Polymeric micelles using cholinium-based ionic liquids for the encapsulation and release of hydrophobic drug molecules. *Biomater Sci*. 9:2183–2196.
- 117 Darani SF, Ahsaie FG, Pazuki G, Abdolrahimi S. 2021. Aqueous two-phase systems based on thermo-separating copolymer for partitioning of doxorubicin. *J Mol Liq*. 322:114542.
- 118 Jiang Y, Chen J, Deng C, Suuronen EJ, Zhong Z. 2014. Click hydrogels, microgels and nanogels: emerging platforms for drug delivery and tissue engineering. *Biomaterials*. 35:4969–4985.
- 119 Zhang X, et al. 2020. Role of a high calcium ion content in extending the properties of alginate dual-crosslinked hydrogels. *J Mater Chem A*. 8:25390–25401.
- 120 Hayes TR, Lyon PA, Silva-Lopez E, Twamley B, Benny PD. 2013. Photo-initiated thiol-ene click reactions as a potential strategy for incorporation of  $[M^1(CO)_3]^+$  ( $M = Re, ^{99m}Tc$ ) complexes. *Inorg Chem*. 52:3259–3267.
- 121 Meldal M, Tomøe CW. 2008. Cu-catalyzed azide–alkyne cycloaddition. *Chem Rev*. 108:2952–3015.
- 122 Baghbanbashi M, Kakkar A. 2021. Polymersomes: soft nanoparticles from Miktoarm stars for applications in drug delivery. *Mol Pharm*. 19:1687–1703.
- 123 Cramer NB, Bowman CN. Thiol-ene and thiol-yne chemistry in ideal network synthesis. In: Lowe A, Bowman C, editors. *Thiol-X chemistries in polymer and materials science*. The Royal Society of Chemistry, Cambridge, UK, 2013. p. 1–27.
- 124 Lowe AB, Hoyle CE, Bowman CN. 2010. Thiol-yne click chemistry: a powerful and versatile methodology for materials synthesis. *J Mater Chem*. 20:4745–4750.
- 125 Matoori S, Leroux JC. 2020. Twenty-five years of polymersomes: lost in translation? *Mater Horizons*. 7:1297–1309.
- 126 Lotocki V, Kakkar A. 2020. Miktoarm star polymers: branched architectures in drug delivery. *Pharmaceutics*. 12:827.
- 127 Sui X, et al. 2015. Robust formation of biodegradable polymersomes by direct hydration. *Polym Chem*. 6:691–696.
- 128 Diaz Bessone MI, et al. 2019. IRGD-guided tamoxifen polymersomes inhibit estrogen receptor transcriptional activity and decrease the number of breast cancer cells with self-renewing capacity. *J Nanobiotechnol*. 17:120.
- 129 Baghbanbashi M, et al. 2022. Stimuli-responsive Miktoarm polymer-based formulations for fisetin delivery and regulatory effects in hyperactive human microglia. *Macromol Biosci*. 22:2200174.
- 130 Lotocki V, et al. 2021. Miktoarm star polymers with environment-selective ROS/GSH responsive locations: from modular synthesis to tuned drug release through micellar partial corona shedding and/or core disassembly. *Macromol Biosci*. 21:2000305.
- 131 Maglio G, et al. 2011. Nanocapsules based on linear and Y-shaped 3-miktoarm star-block PEO-PCL copolymers as sustained delivery system for hydrophilic molecules. *Biomacromolecules*. 12:4221–4229.
- 132 Lee James CM, et al. 2001. Preparation, stability, and in vitro performance of vesicles made with diblock copolymers. *Biotechnol Bioeng*. 73:135–145.
- 133 Hashemi M, Kalalinia F. 2015. Application of encapsulation technology in stem cell therapy. *Life Sci*. 143:139–146.
- 134 Zhang X, et al. 2019. Comparative analysis of droplet-based ultra-high-throughput single-cell RNA-seq systems. *Mol Cell*. 73:130–142.e5.
- 135 Chong DT, et al. 2015. Advances in fabricating double-emulsion droplets and their biomedical applications. *Microfluid Nanofluidics*. 19(19):1071–1090.
- 136 Yaakov N, et al. 2018. Single cell encapsulation via pickering emulsion for biopesticide applications. *ACS Omega*. 3:14294–14301.
- 137 Brower KK, et al. 2020. Double emulsion picoreactors for high-throughput single-cell encapsulation and phenotyping via FACS. *Anal Chem*. 92:13262–13270.
- 138 Cheng R, Meng F, Deng C, Klok HA, Zhong Z. 2013. Dual and multi-stimuli responsive polymeric nanoparticles for programmed site-specific drug delivery. *Biomaterials*. 34:3647–3657.
- 139 Das SS, et al. 2020. Stimuli-responsive polymeric nanocarriers for drug delivery, imaging, and theragnosis. *Pharmaceutics*. 12:1397.
- 140 Fu X, Hosta-Rigau L, Chandrawati R, Cui J. 2018. Multi-stimuli-responsive polymer particles, films, and hydrogels for drug delivery. *Chem*. 4:2084–2107.
- 141 Cheng W, Gu L, Ren W, Liu Y. 2014. Stimuli-responsive polymers for anti-cancer drug delivery. *Mater Sci Eng C*. 45:600–608.
- 142 Sampath Udeni Gunathilake TM, Ching YC, Chuah CH, Rahman NA, Liou NS. 2020. Recent advances in celluloses and their hybrids for stimuli-responsive drug delivery. *Int J Biol Macromol*. 158:670–688.
- 143 Bami MS, Raeisi Estabragh MA, Khazaeli P, Ohadi M, Dehghannoudeh G. 2022. pH-responsive drug delivery systems as intelligent carriers for targeted drug therapy: brief history, properties, synthesis, mechanism and application. *J Drug Deliv Sci Technol*. 70:102987.
- 144 Li S, Zhang R, Wang D, Feng L, Cui K. 2021. Synthesis of hollow maghemite ( $-Fe_2O_3$ ) particles for magnetic field and pH-responsive drug delivery and lung cancer treatment. *Ceram Int*. 47:7457–7464.
- 145 Karimi S, Namazi H. 2021.  $Fe_3O_4$ @PEG-coated dendrimer modified graphene oxide nanocomposite as a pH-sensitive drug carrier for targeted delivery of doxorubicin. *J Alloys Compd*. 879:160426.
- 146 Taghizadeh B, et al. 2015. Classification of stimuli-responsive polymers as anticancer drug delivery systems. *Drug Deliv*. 22: 145–155.
- 147 Li Y, Ding J, Zhu J, Tian H, Chen X. 2018. Photothermal effect-triggered drug release from hydrogen bonding-enhanced polymeric micelles. *Biomacromolecules*. 19:1950–1958.
- 148 Wang D, et al. 2011. Supramolecular copolymer micelles based on the complementary multiple hydrogen bonds of nucleobases for drug delivery. *Biomacromolecules*. 12:1370–1379.
- 149 Yao P, et al. 2021. Construction and characterization of a temperature-responsive nanocarrier for imidacloprid based on mesoporous silica nanoparticles. *Colloids Surfaces B Biointerfaces*. 198:111464.
- 150 Kitano K, Ishihara K, Yusa SI. 2022. Preparation of a thermo-responsive drug carrier consisting of a biocompatible triblock copolymer and fullerene. *J Mater Chem B*. 10:2551–2560.
- 151 Asgari M, Soleymani M, Miri T, Barati A. 2021. Design of thermo-sensitive polymer-coated magnetic mesoporous silica nanocomposites with a core-shell-shell structure as a magnetic/temperature dual-responsive drug delivery vehicle. *Polym Adv Technol*. 32:4101–4109.
- 152 Andreeva DV. *Adv Ave Dev Nov Carriers Bioact Biol Agents*. Academic Press San Diego, CA, 2020. p. 183–209.
- 153 Xu W, Steinschulte AA, Plamper FA, Korolovych VF, Tsukruk VV. 2016. Hierarchical assembly of star polymer polymersomes into responsive multicompartamental microcapsules. *Chem Mater*. 28:975–985.
- 154 Gelissen APH, Pergushov DV, Plamper FA. 2013. Janus-like interpolyelectrolyte complexes based on miktoarm stars. *Polymer (Guildf)*. 54:6877–6881.
- 155 Bajpai AK, Shukla SK, Bhanu S, Kankane S. 2008. Responsive polymers in controlled drug delivery. *Prog Polym Sci*. 33:1088–1118.
- 156 Hajebi S, et al. 2019. Stimulus-responsive polymeric nanogels as smart drug delivery systems. *Acta Biomater*. 92:1–18.